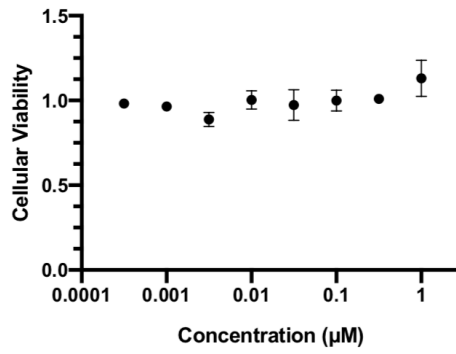
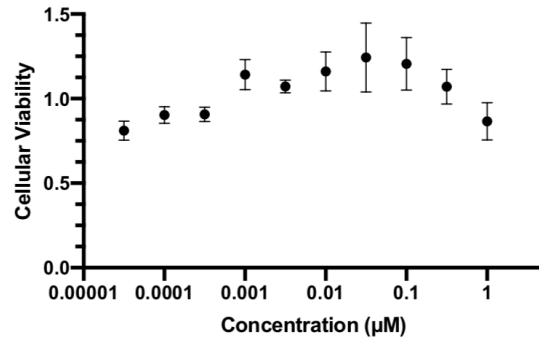


**Figure S1: Effect of LCL161 on viability of MC38 cells** (related to figure 5)  
Viability of MC38 cells after LCL161 treatment for 24 hours (a) and for 1 week (b). Data is normalized to DMSO control. N = 3 points per dose. Reported is mean +/- S.D.

**a**



**b**



**Figure S2: Localization of Nanoparticle to tumor associated macrophages (TAM)** (related to figure 6)

Nanoparticles primarily accumulate to a much higher degree in tumor associated macrophages. (a). Co-localization analysis of nanoparticle image channel against tumor channel (left) or macrophage channel (right). Plotted are Pearson correlation values. Higher values of correlation indicate more co-localization, indicating that nanoparticles and TAM co-localize well. N = 13 images, reported are mean  $\pm$  S.D. ( $p < 0.0001$ , t-test with Welch's correction) (b). Distribution of mean fluorescent intensity of CDNP nanoparticle in tumor cells and macrophages. Tumor associated macrophages have substantially higher, but also heterogenous levels of CDNP uptake ( $p < 0.0001$ , Kolmogorov-Smirnov test).

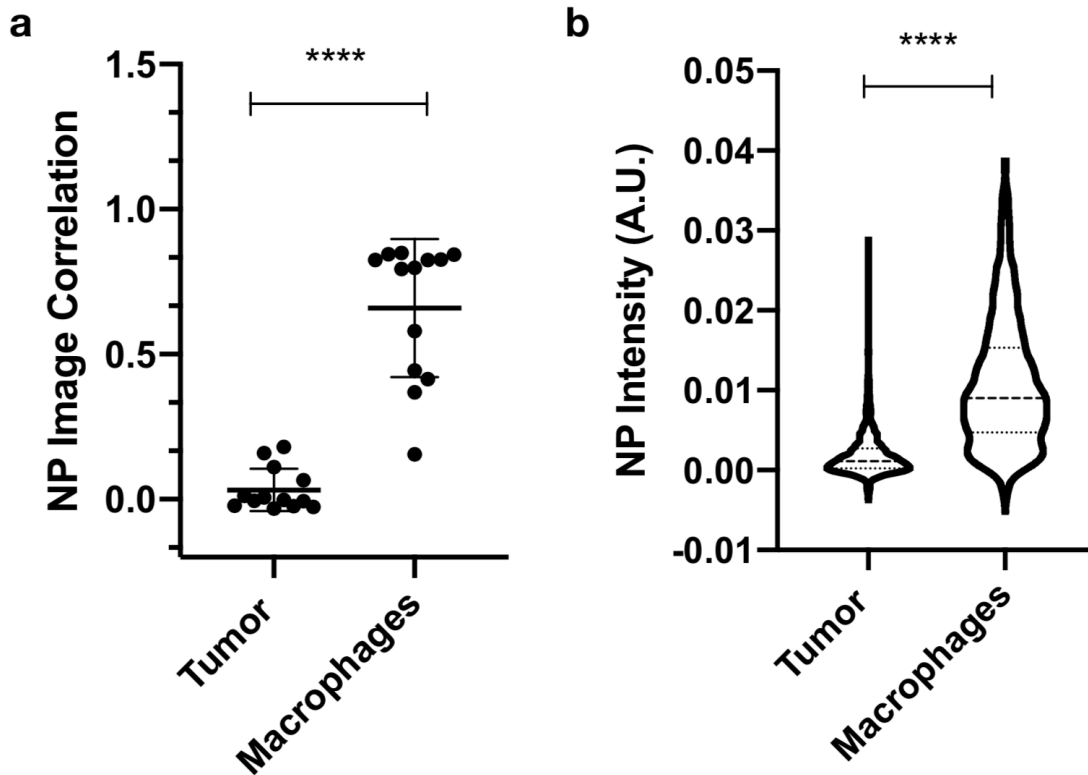


**Figure S3: Distribution of IL-12 positive cells in tumor and LNs** (related to figure 6)

a. Hindlimb tumors, tumor draining lymph nodes, and non-draining axillary lymph nodes were harvested, and scanned for IL12-eYFP signal. Both tumors and draining lymph nodes had strong presence of eYFP+ cells but no signal was observed in non-draining distal lymph nodes.  
b. Quantification of data in (a). N = 2, reported is mean  $\pm$  S.D. (c). Confocal imaging of tumor, inguinal, and axillary lymph nodes. (Green = eYFP immune cells, red = MC38 tumor cells, blue = Macrophages).

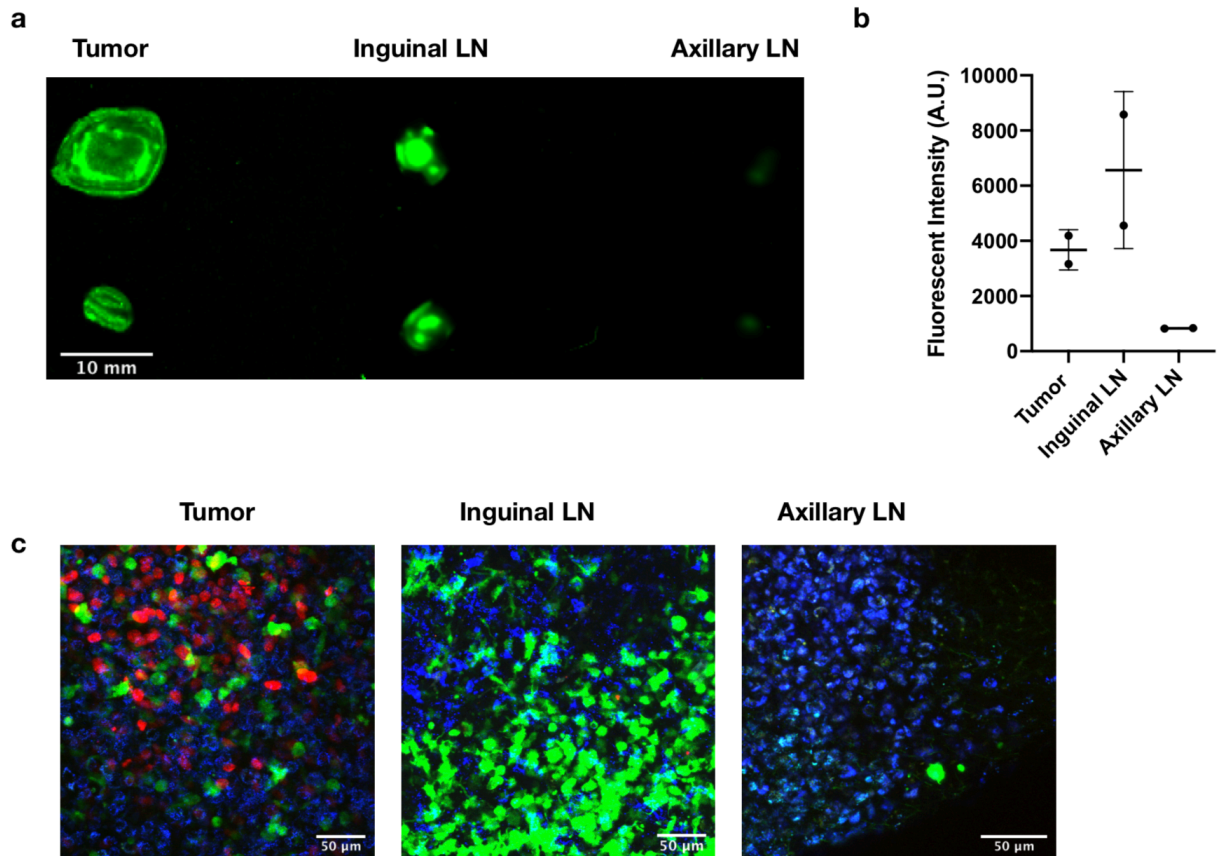


**Figure S4: Histology of Liver and Spleen** (related to figure 5)

Representative H&E images of liver (a), and spleen (b) from mice treated with either saline, empty CDNP, LCL161-CD (free drug), or LCL161-CDNP. No histologically observable toxicity or excessive immune infiltrates were evident in any of the groups.

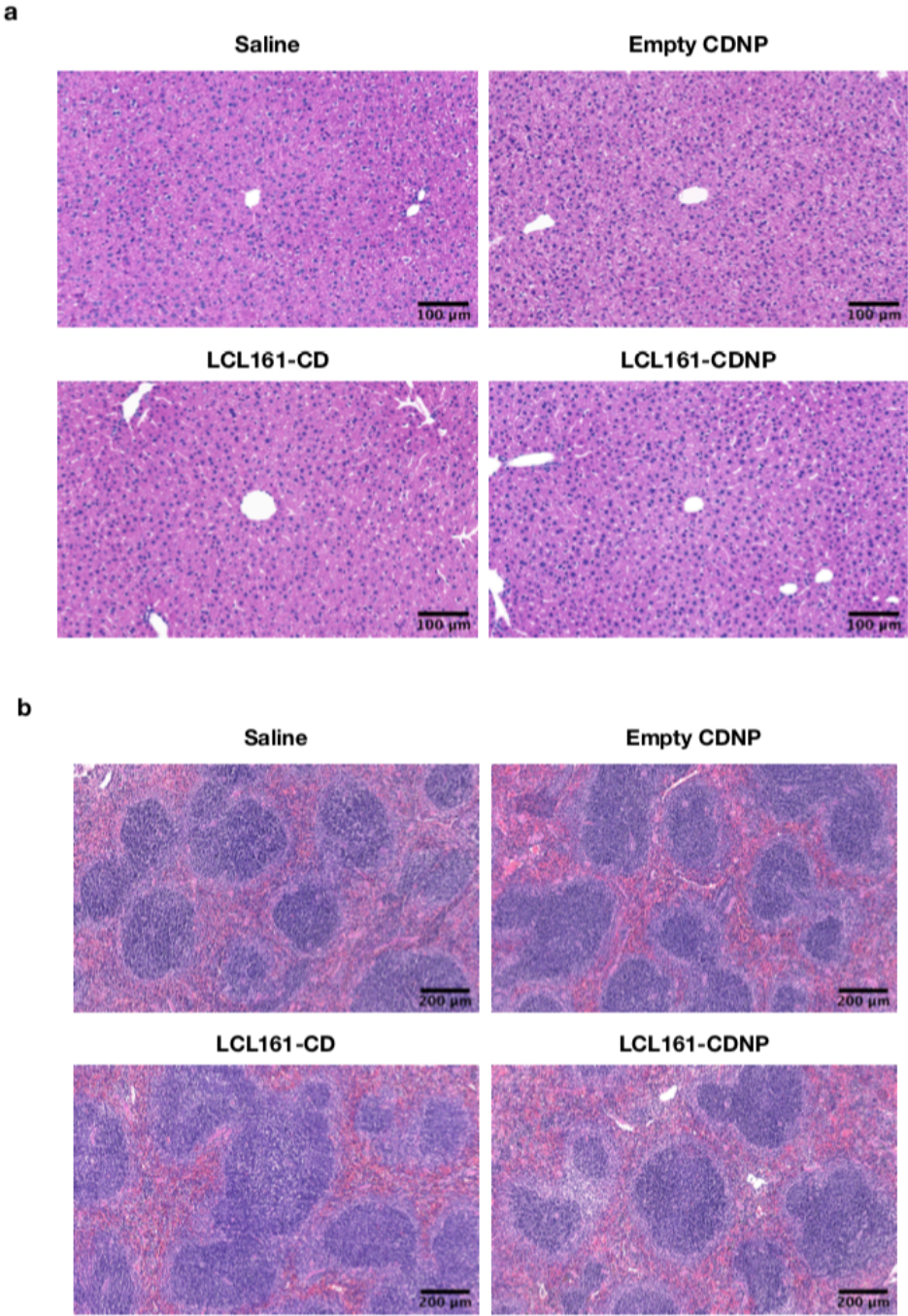


**Figure S5: Organ Weights** (related to figure 5)

Weights of organs harvested one day after treatment with either saline, empty CDNP, LCL161-CD, or LCL161-CDNP. There was no statistically significant decreases in organ weights as would be expected with acute toxicity. Slight increases were seen in the small intestines of mice treated with LCL161-CD and LCL161-CDNP (Two way ANOVA, Tukey's Multiple Comparison Test). Reported is mean +/- S.D, N = 2 mice per group.

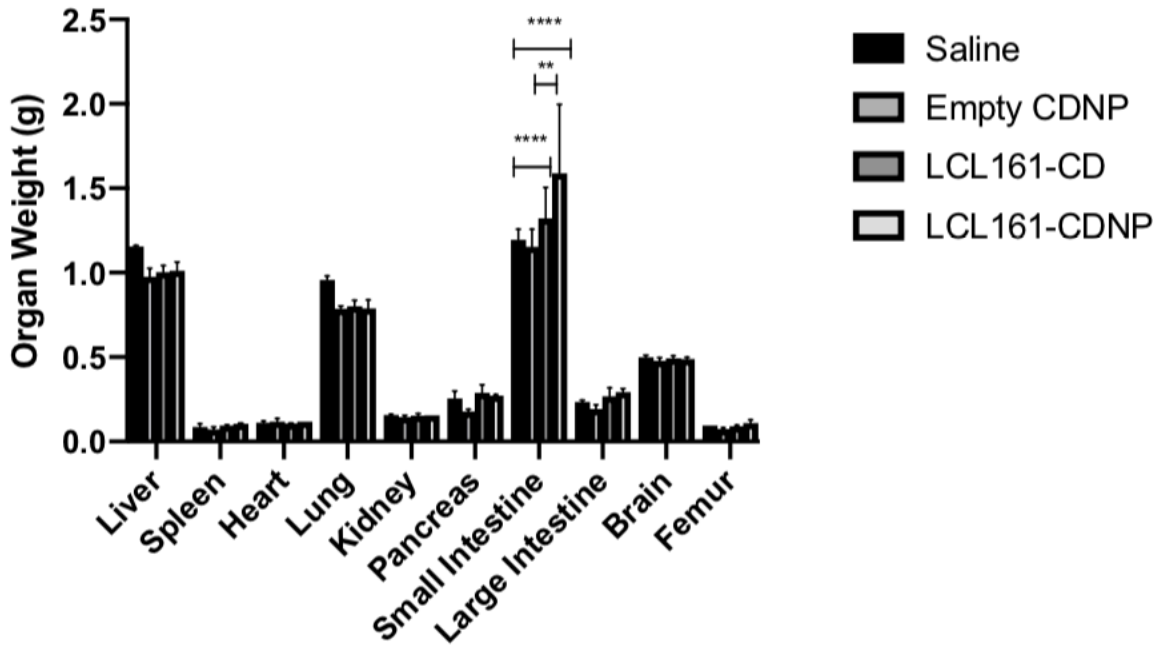
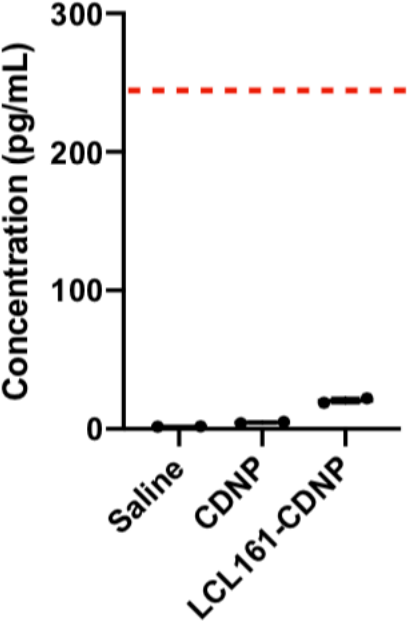


**Figure S6: Serum IL-12 Measurements** (related to figure 5)  
Measurement of IL-12 serum levels in mice treated with saline, empty CDNP, or LCL161-CDNP (N=6, Reported as mean  $\pm$  S.D.). Mild elevation of IL-12 is seen in LCL161-CDNP treated mice but this is below what is seen with toxic stimuli, such as staphylococcal enterotoxin A (dashed red line) (Abdi et al., 2018, J Immunol, 201, 2879-2884)

### IL-12 Serum Concentration



**Movie S1. Intravital imaging of IL12-eYFP expressing cells.** (related to figure 6)

To examine the distribution and behavior of activated myeloid cells, intravital confocal microscopy was performed in p40-IRES-eYFP mice at 24 hours following administration of VT680 labeled LCL161-CDNP. A large population of sessile dextran positive cells (predominantly macrophages) is observed to produce low levels of IL12. A second population of highly motile dextran negative cells (predominantly DCs) is observed produce high levels of IL12. Green: eYFP (IL12+ immune cells), red: MC38-H2B-mApple (tumor cells), blue: Pacific blue dextran (macrophages), white: VT680 (CDNP).